Supporting Information

Rodriguez-Menchaca et al. 10.1073/pnas.1207901109

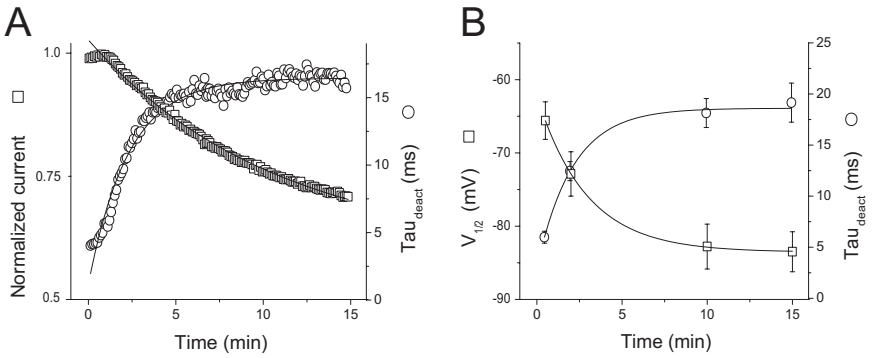

Fig. S1. Distinct kinetics of the current rundown and of the gating shift of Kv1.2 channels recorded in ND96K under inside–out patch conditions. (*A*) Time constants for Kv1.2 current rundown (squares) and deactivation kinetics (τ_{deact}) (circles). Lines are fits of a single exponential function to the data with values for time constant (τ) of 10.68 ± 0.27 min and 2.3 ± 0.1 min for rundown and τ_{deact} respectively. (*B*) Time constants for the midpoint of voltage activation ($V_{1/2}$) and τ_{deact} as a function of time. Data adjusted to a single exponential gave a time constant (τ) of 2.9 ± 1.9 min and 2.9 ± 0.6 min for $V_{1/2}$ and τ_{deact}, respectively. Data shown are ± SEM; n = 4.

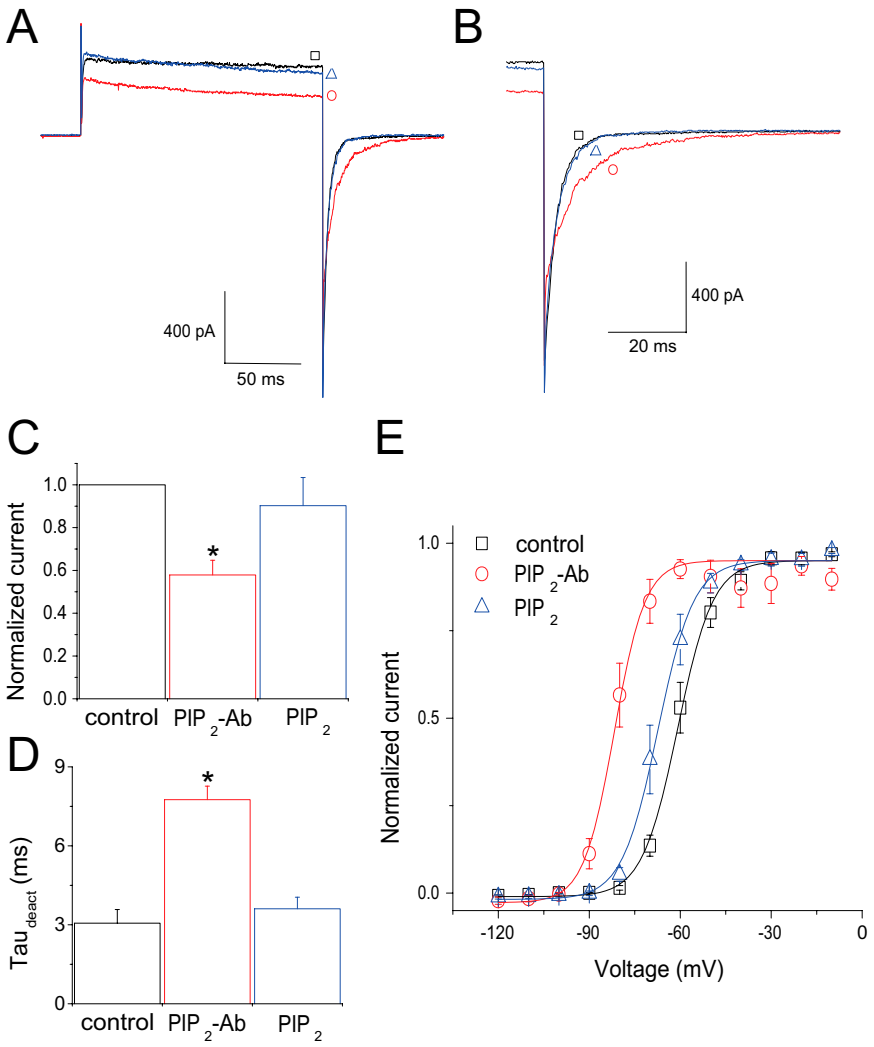

Fig. S2. PIP_2-Ab–mediated effects on voltage-dependent gating and current amplitude of *Shaker* channels are reversed by PIP_2, just as in Kv1.2 channels. (*A*) Representative traces showing effects of PIP_2-Ab (blue) and PIP_2 (red) on currents in *Shaker* channels in which the inactivation domain was removed (Shk-IR). Black trace represents control channel. (*B*) Deactivation of Shk-IR tail currents in control channels (black) and with PIP_2-Ab (red) and PIP_2 (blue) application. (*C*) Summary of the effects of PIP_2-Ab and PIP_2 on current amplitude. Data shown are ± SEM; $n = 5$. (*D*) Summary of the time constants of deactivation (τ_{deact}) from tail currents, similar to those shown in *B*, in control channels and with PIP_2-Ab or PIP_2 application. Data shown are ± SEM; $n = 5$. (*E*) Steady-state activation curves of *Shaker* channels determined before (control, black) and after application of 10 μg/mL PIP_2-Ab (red) and during subsequent application of 10 μM PIP_2 (blue). Data points are mean ± SEM; $n = 5$. Lines are fits of a Boltzmann function to the data. $^*P < 0.05$ versus control.

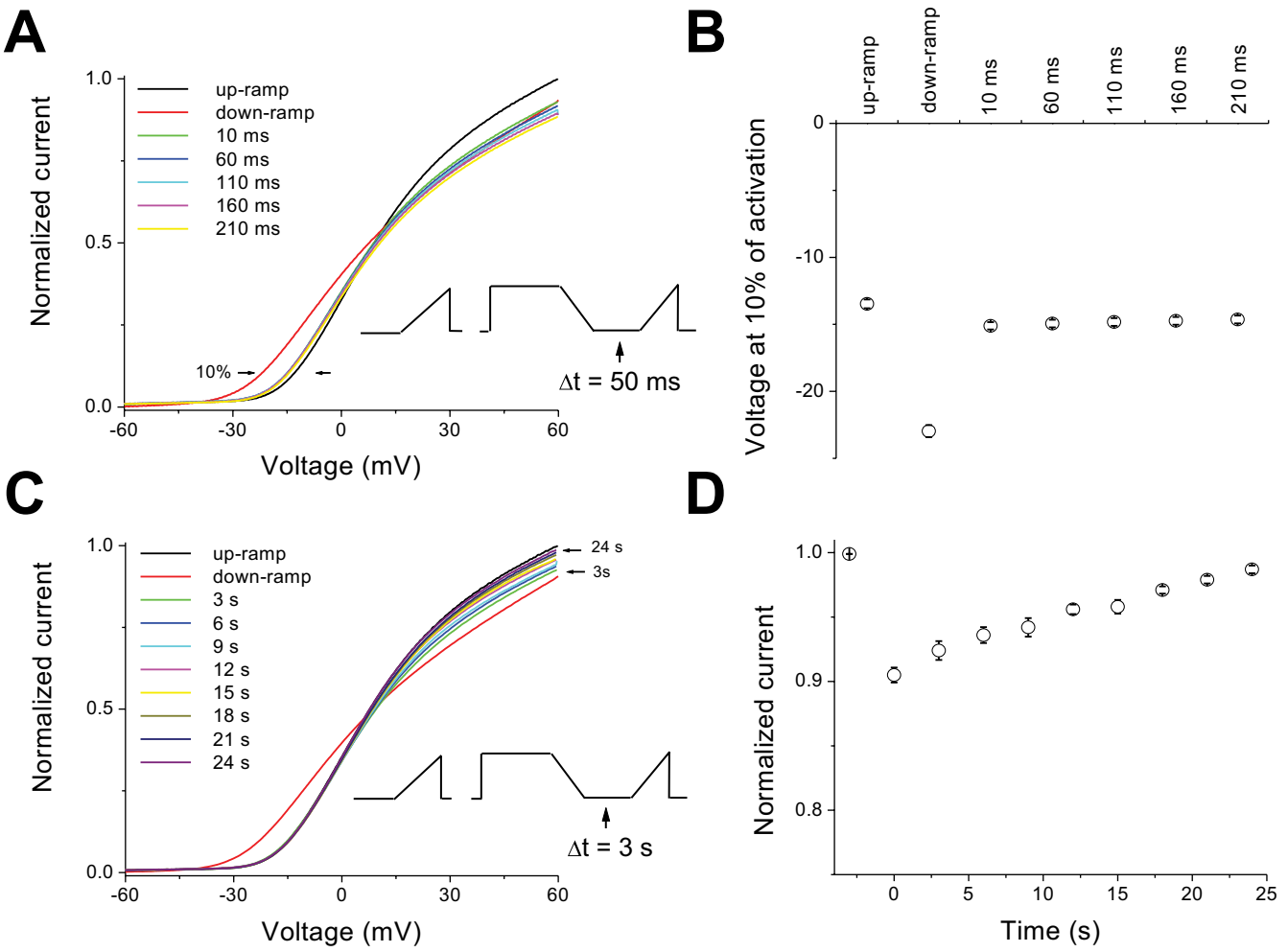

Fig. S3. Distinct recovery kinetics of the shift in voltage dependence and change in current amplitude following PIP_2 depletion by *Ciona intestinalis* voltage-sensitive phosphatase (Ci-VSP). (*A*) Representative current–voltage relationships of Kv1.2 channels coexpressed with Ci-VSP evoked by the protocol illustrated in the *Inset*. (*B*) Temporal course of the shift recovery as a function of the repolarization duration. Data shown are ± SEM; $n = 5$. (*C*) Representative current–voltage relationships of Kv1.2 channels coexpressed with Ci-VSP evoked by the protocol illustrated in the *Inset*. (*D*) Temporal course of current amplitude recovery as a function of the repolarization duration. Data shown are ± SEM; $n = 5$.

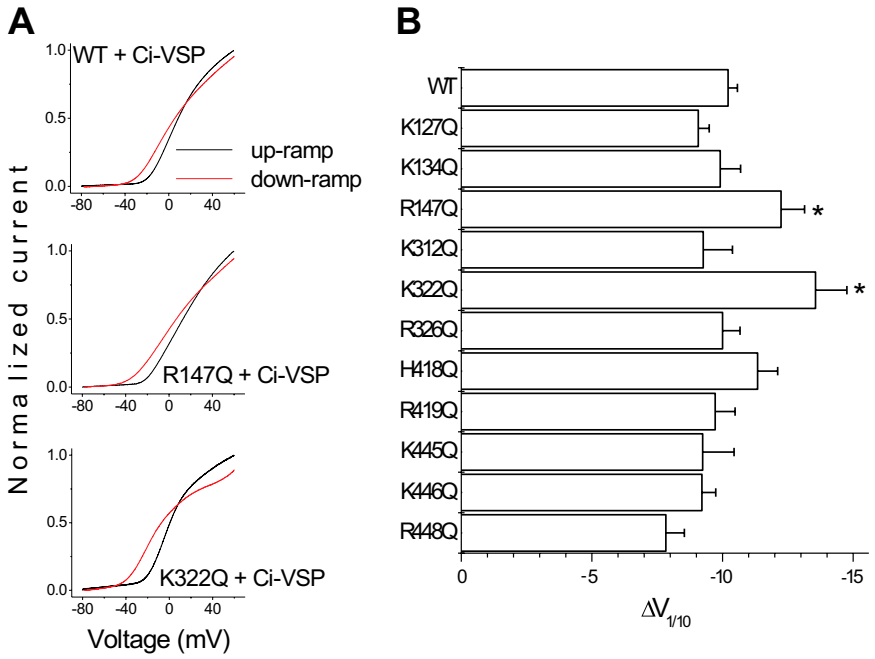

Fig. S4. Scanning mutagenesis of Kv1.2 positively charged residues reveals distinct determinants of PIP_2 effects on the voltage-dependent shift, using Ci-VSP. (*A*) Representative current–voltage relationships of Kv1.2 channels coexpressed with Ci-VSP from recordings performed using the protocols shown in Fig. S4 for wild-type and mutant channels (R147Q, and K322Q). (*B*) The difference in the voltage at 10% of activation ($\Delta V_{1/10}$) for Kv1.2 wild-type and mutant channels. The differences in $\Delta V_{1/10}$ between wild-type and R147Q and between wild-type and K322Q channels were statistically significant (*$P < 0.05$). Data shown are ± SEM; n = 5–6.

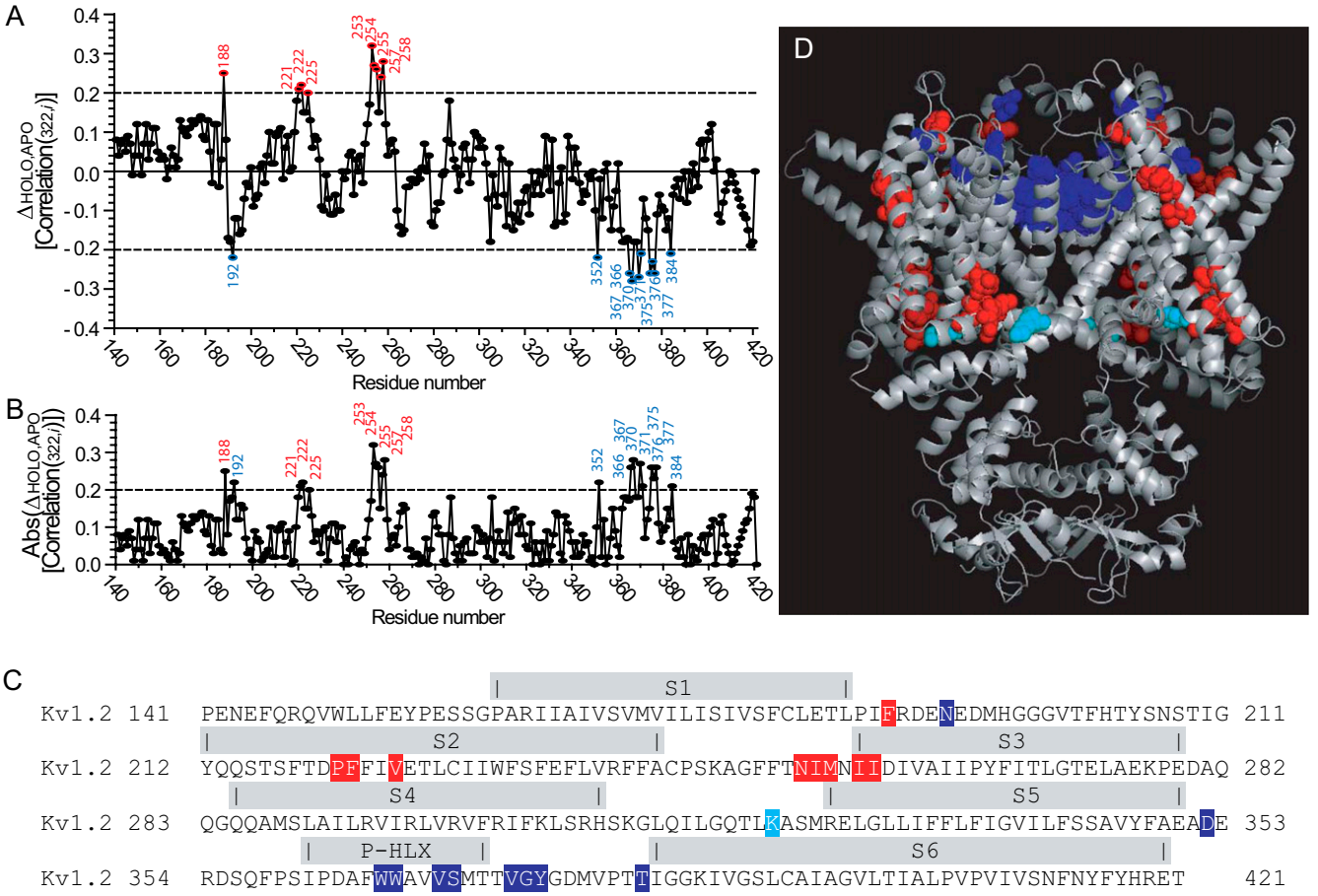

Fig. S5. Changes in the correlated motions of K322 with the transmembrane residues in the presence of PIP_2. Correlation analysis was conducted on trajectories of 50–100 ns in the presence and absence of PIP_2. Correlation values range between −1 and 1. The larger the absolute value of the correlation between two residues, the larger is their correlation. Using K322 to represent the S4–S5 linker, we calculated the correlation between K322 and all transmembrane residues in the presence and absence of PIP_2. The differences in these correlations with and without PIP_2 are depicted in *A* as a function of the transmembrane residue number. *B* depicts the absolute values of the differences shown in *A*. The residues that exhibit maximal absolute differences (≥0.2) in the correlated motions are labeled on both panels, and their location in the sequence is shown in *C*. Residues colored red exhibit maximal increased correlation in the presence of PIP_2. Residues colored blue exhibit maximal decreased correlation. These residues are shown with the same color-coding in a 3D model of the open channel conformation in *D*.